J Mater Sci: Mater Med (2008) 19:2953–2962
DOI 10.1007/s10856-008-3413-6

# Surface modification of polydimethylsiloxane (PDMS) induced proliferation and neural-like cells differentiation of umbilical cord blood-derived mesenchymal stem cells

**Sun-Jung Kim · Jae Kyoo Lee · Jin Won Kim · Ji-Won Jung · Kwangwon Seo · Sang-Bum Park · Kyung-Hwan Roh · Sae-Rom Lee · Yun Hwa Hong · Sang Jeong Kim · Yong-Soon Lee · Sung June Kim · Kyung-Sun Kang**

Received: 6 September 2007 / Accepted: 22 February 2008 / Published online: 24 March 2008


**Abstract** Stem cell-based therapy has recently emerged for use in novel therapeutics for incurable diseases. For successful recovery from neurologic diseases, the most pivotal factor is differentiation and directed neuronal cell growth. In this study, we fabricated three different widths of a micro-pattern on polydimethylsiloxane (PDMS; 1, 2, and 4 μm). Surface modification of the PDMS was investigated for its capacity to manage proliferation and differentiation of neural-like cells from umbilical cord blood-derived mesenchymal stem cells (UCB-MSCs). Among the micro-patterned PDMS fabrications, the 1 μm-patterned PDMS significantly increased cell proliferation and most of the cells differentiated into neuronal cells. In addition, the 1 μm-patterned PDMS induced an increase in cytosolic calcium, while the differentiated cells on the flat and 4 μm-patterned PDMS had no response. PDMS with a 1 μm pattern was also aligned to direct orientation within 10° angles. Taken together, micro-patterned PDMS supported UCB-MSC proliferation and induced neural like-cell differentiation. Our data suggest that micro-patterned PDMS might be a guiding method for stem cell therapy that would improve its therapeutic action in neurological diseases.

S.-J. Kim and J. K. Lee contributed equally to this work.

**Electronic supplementary material** The online version of this article (doi:10.1007/s10856-008-3413-6) contains supplementary material, which is available to authorized users.

S.-J. Kim · J.-W. Jung · K. Seo · S.-B. Park · K.-H. Roh · S.-R. Lee · Y.-S. Lee · K.-S. Kang (✉)
Adult Stem Cell Research, College of Veterinary Medicine, Seoul National University, 151-742 Seoul, Republic of Korea
e-mail: kangpub@snu.ac.kr

S.-J. Kim · J.-W. Jung · K. Seo · S.-B. Park · K.-H. Roh · S.-R. Lee · Y.-S. Lee · K.-S. Kang
Laboratory of Stem Cell and Tumor Biology, Department of Veterinary Public Health, College of Veterinary Medicine, and BK21 Program for Veterinary Science, Seoul National University, 151-742 Seoul, Republic of Korea

J. K. Lee · J. W. Kim · S. J. Kim
Nano-Bio-Electronics & System Research Center, Seoul National University, 151-742 Seoul, Republic of Korea

J. W. Kim · S. J. Kim (✉)
School of Electrical Engineering & Computer Science, Seoul National University, 151-742 Seoul, Republic of Korea
e-mail: kimsj@snu.ac.kr

Y. H. Hong · S. J. Kim
Laboratory of Neurophysiology, Seoul National University College of Medicine, 151-742 Seoul, Republic of Korea

## 1 Introduction

Recently, it has been demonstrated that mesenchymal stem cells (MSCs) from various tissues, such as the bone marrow [1], umbilical cord [2], and adipocyte tissue [3], have multipotent abilities to undergo osteogenic, adipogenic, hepatocyte, and neuronal differentiation [4, 5]. These findings have raised interest in umbilical cord blood-derived mesenchymal stem cells (UCB-MSCs) as potential sources for support of clinical treatments [6, 7]. We have reported successful clinical trials of MSCs from cord blood used for Buerger's disease and ischemic limb disease in vivo [8] and UCB-MSCs have been induced into insulin-producing islet-like structures in vitro [9]. Fu et al. [10] also suggested that MSCs from cord blood have potential in the treatment of Parkinson's disease. To enhance the therapeutic effect of stem cells, one prerequisite is high proliferation and differentiation towards desired lineages of MSCs. However, stem cell-based therapy usually does not efficiently result in cell proliferation and differentiation to levels high enough

for the curing of incurable diseases [11]. For the successful treatment of neurological disorders, neuronal cells require directed neuronal outgrowth and neuronal differentiation [12]. Therefore, many different types of biomaterials have been used as environments for the regeneration of neurological disorders, including hydrogel, poly D,L,lactic-co-glycolde (PLGA), polystyrene, and polydimethylsiloxane (PDMS) [12–14]. Moreover, physical modification of biomaterials, such as surface patterning and topography, has also influenced cell proliferation, positioning, and differentiation [15–17]. One of these biomaterials, PDMS, is widely known as an appropriate material not only for surface patterning and topographic modification, but also as a good substrate for cell growth, proliferation, and differentiation due to the its mechanical stability, biocompatibility, and non-toxicity [18–20].

In this study, we hypothesized that a microstructure on PDMS material would influence the proliferation of UCB-MSCs and their differentiation into neuronal cells by controlling their orientation. This study demonstrated that physical cues added to the PDMS played important roles in the proliferation and differentiation of UBC-MSCs. We fabricated different widths of micro-patterns (1, 2, and 4 μm) on PDMS to investigate UCB-MSC proliferation and neuronal differentiation.

## 2 Materials and methods

### 2.1 PDMS and micro-patterned fabrication

Micro-scale surface topographies were fabricated on PDMS from a silicon mold. The silicon mold was fabricated by photolithography and etching techniques. A series of microgrooves, 1, 2, or 4 μm in width and 1 μm in height, was fabricated on silicon wafers. The silicon wafers were cleaned using $H_2SO_4/H_2O_2$ (4:1), HF, and distilled water cleaning processes. A Sylgard 184 PDMS elastomer (Dow Corning, Midland, MI, USA) was used for cell culture substrata. A Sylgard 184 hardener was added to the Sylgard 184 PDMS base at a ratio of 1:10 before it was poured into the silicon mold. After the PDMS was poured into the silicon templates, the PDMS and mold were transferred into a vacuum chamber for degassing. Afterwards, the PDMS attached to the silicon mold was heated on a hot plate for 1 h at 70°C for hardening. The PDMS layers were gently peeled from the silicon molds, and complimentary replicas with grooved topographies were generated on the PDMS surfaces. Supplementary Figure 1 shows the resulting microstructure fabricated on the PDMS substrate. These PDMS substrata were washed in an ultrasonic cleaner bath for 15 min to remove particles from the PDMS surface. These PDMS samples were sterilized with 70% EtOH and UV irradiation and a Poly-D-Lysin (PDL) coating prior to the seeding of the cells.

### 2.2 Culture for human MSCs

Human UCB samples were obtained from Seoul Cord Blood Bank (Seoul, Korea); samples from term and preterm deliveries were harvested at the time of birth with the consent of the mother. This work was approved by the Borame Hospital Institutional Review Board (IRB) and the Seoul National University IRB. Blood samples were processed within 24 h of collection. The mononuclear cells were separated from the UCB using Ficoll-PaqueTM PLUS (Amersham Bioscience, Uppsala, Sweden) and suspended in culture medium (DEME; Gibco, Grand Island, NY, USA) containing 20% FBS, 100 U/ml penicillin, 100 mg/ml streptomycin, 2 mM L-glutamine, and 1 mM sodium pyruvate. The cells were then seeded at a density of $1 \times 10^6$ cells/cm$^2$ in culture flasks. After 7 days of culture, the suspended cells were removed and the adherent cells were additionally cultured using previously reported methods [8]. Cells were maintained at 37.8°C in a humidified atmosphere containing 5% $CO_2$, with a change of culture medium every 3–4 days. Approximately 50–60% of the confluent cells were detached with 0.2% trypsin-EDTA and replated at a density of $2 \times 10^3$ cells/cm$^2$ in culture flasks.

### 2.3 Neuronal differentiation of UCB-human (h)MSCs

The method of neuronal differentiation was followed, as modified by Kang et al. [4]. When hMSCs derived from UCB reached approximately 50–60% confluence, the medium was changed to DMEM containing 1 mM BME and 5% FBS for 24 h. Cells were exposed to another new medium, 1% DMSO and 100 μM BHA in DMEM. After 5 h, cells were fixed with 4% paraformaldehyde in PBS for immunostaining or loaded with 5 μM Fura 2 and 0.01% of Pluronic F-127 acid in HBSS for calcium imaging.

### 2.4 Immunostaining

Fixed MSCs or neuronal differentiated cells were permeablized in 0.02% TritonX-100 and then blocked with 10% normal goat serum (NGS) for 1 h. After the blocking step, the first antibody, $\beta$ III tubulin (1:200; Covance, Berkley, CA, USA) was added into the cells, which were then incubated for 1 day at 4°C. Cells were rinsed three times with 1X PBS, and were then incubated with the second antibody, Alexa 488 (1:1000, Molecular Probe, Inc., Eugene, OR, USA) for 1 h. Finally, for nuclear staining, Hoechst 33238 (1 μg/ml) was diluted 1:100 in PBS and loaded into samples for 15 min. Images were captured on a confocal microscope (Eclipse TE200; Nikon, Japan).

### 2.5 Calcium imaging

To evaluate calcium imaging of differentiated neurons on PDMS, cells were loaded with a calcium indicator dye (5 μM of Fura 2; Molecular Probe, Inc.) and 0.01% of Pluronic F-127 acid in HBSS for a 45 min incubation at 37°C. Cells were placed on the stage of a microscope equipped with water immersion and a confocal head (Olympus, Japan). Perfusion with 133 mM KCl and HBSS buffer was performed in the water bath using a muti-valve process. Each frame was captured every 5 s. Calcium relative changes were expressed as F (340 nm)/F0 (380 nm). Data acquisition and calcium imaging were performed with the Imaging Workbench 2.1 program (Axon Instruments, Inc., USA).

### 2.6 Measurement of cell alignment

After induction of neuronal differentiation of the UCB-MSCs, the cells were fixed, labeled, and transferred to a confocal microscope for immunostaining imaging. The images of differential interference contrast (DIC) and fluorescence of Hoechst 33238 and $\beta$ III tubulin-positive cells were captured by confocal microscopy. The captured images of DIC, Hoechst, and $\beta$ III tubulin were merged into one image for further measurements. A straight line from the one longest chord of a cell to the other end of the chord was determined for each cell on the merged images. The alignment of cells was determined by measuring the angle between the straight line and an axis of the grooves on the surface. The parallel direction with respect to the axis of the grooves was defined as 0°. The measured data were grouped in 10° sectors from 0 to 90°. The 0° indicated perfect alignment to the microgrooves. Statistical analysis was performed for the measured groups of orientations for each scale of grooves (1, 2, and 4 μm). The frequencies of the cells aligned within 10 and 20° with respect to the grooves were analyzed.

### 2.7 Scanning electron microcopy

Neuronally differentiated cells on PDMS were fixed in 4% paraformaldehyde and dehydrated in a graded alcohol series. At the critical point, they were dried with $CO_2$ (BAL-TEC, Arizona, USA), followed by coating with gold plates (JEOL, Tokyo, Japan). Samples were then examined under a scanning electron microscopy (SEM) (JEOL).

### 2.8 Statistical analysis

Statistical analysis was performed using ANOVA followed by Duncan's multiple range tests ($P < 0.05$).

## 3 Results

### 3.1 Micro-patterned PDMS fabrication

As shown in Fig. 1, SEM images for the micro-scale surface topographies fabricated on PDMS from silicon molds showed patterned PDMS with 1 (a), 2 (b), and 4 μm patterns (c) and a flat PDMS.

### 3.2 Micro-patterned PDMS enhanced the proliferation of cord blood-derived MSCs

Before our investigation into whether micro-patterned PDMS affects cell growth and behavior, we evaluated the capacity of UCB-hMSC proliferation in PDMS and commercial plastic dishes with PDL coating by cell counting. Even though there was no significant difference, UCB-hMSCs were more proliferative in PDMS than in commercial plastic dishes (Fig. 2a) and adherent UCB-hMSCs on PDMS continuously increased until confluence. This data indicated that PDMS was a good substrate for cell growth. To evaluate the proliferation of UCB-hMSCs on the modified surface of PDMS, UCB-hMSCs were plated on micro-patterned and flat PDMS (Fig. 2b). We also tested apoptotic and necrotic cell death of UCB-MSCs on the micro-patterned PDMS. We performed double staining with Hoechst 33238 and propidium iodide (PI). Hoechst 33238 is a marker of apoptosis of cells with fragmented and/or condensed nuclei and PI is an indicator of necrotic cell death. We did not detect any necrotic (PI staining was negative) or apoptotic cell death with condensed and/or fragmented nuclei on PDMS of the UCB-hMSCs (Fig. 3). When comparing the UCB-hMSCs on patterned PDMS and PDMS without any pattern, dramatically more proliferation of UCB-hMSCs occurred in micro-patterned PDMS than in flat PDMS. PDMS with a 1 μm pattern induced cell proliferation about 2-fold that of the flat PDMS (Fig. 2b). Most of the micro-patterned PDMS increased the proliferation of the UCB-hMSCs, but there was no statistical significance between the flat and 4 μm pattern of PDMS (Fig. 2b).

### 3.3 UBC-hMSCs were highly differentiated into neural-like cells on micro-patterned PDMS

We determined whether the microstructure of PDMS could affect neural-like cell differentiation of UCB-hMSC cells. UCB-hMSCs were seeded at a density of 50,000 cells/ml in DMEM containing 20% of FBS on the fabricated PDMS. When cells reached 50–60% confluence (Fig. 4a), the medium was replaced with pre-neuronal induction medium for 24 h (Fig. 4b). The medium was again

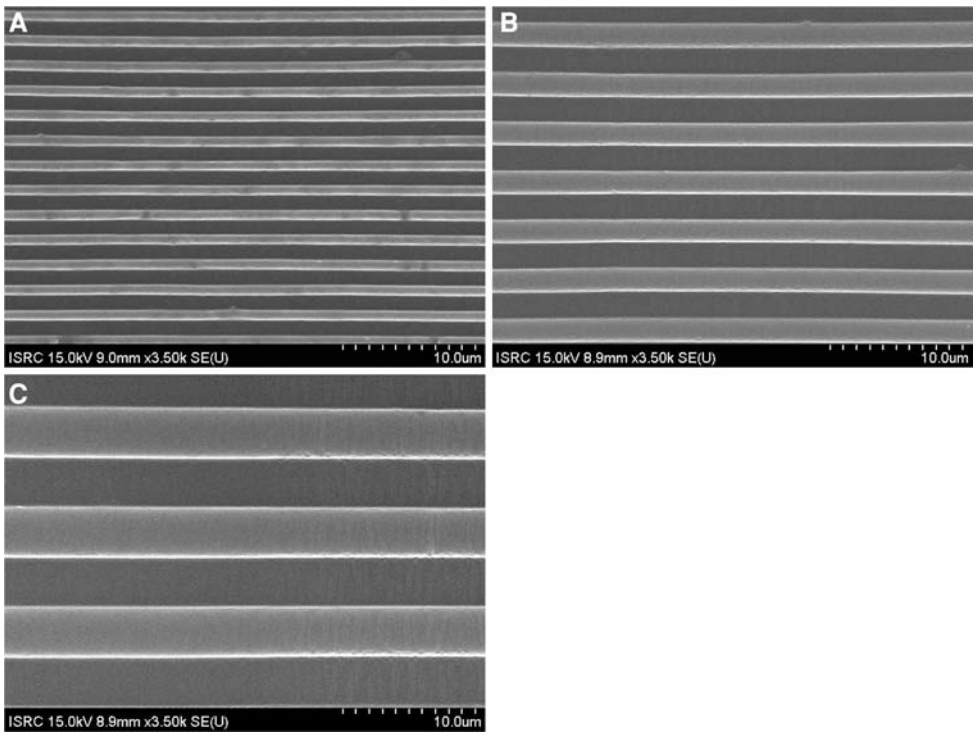


**Fig. 1** Topographies on PDMS by SEM image analysis. Micro-patterned PDMS were fabricated using silicon molds. (**a**) PDMS with 1 μm pattern, (**b**) PDMS with 2 μm pattern, and (**c**) PDMS with 4 μm pattern (Scale bar = 10 μm)

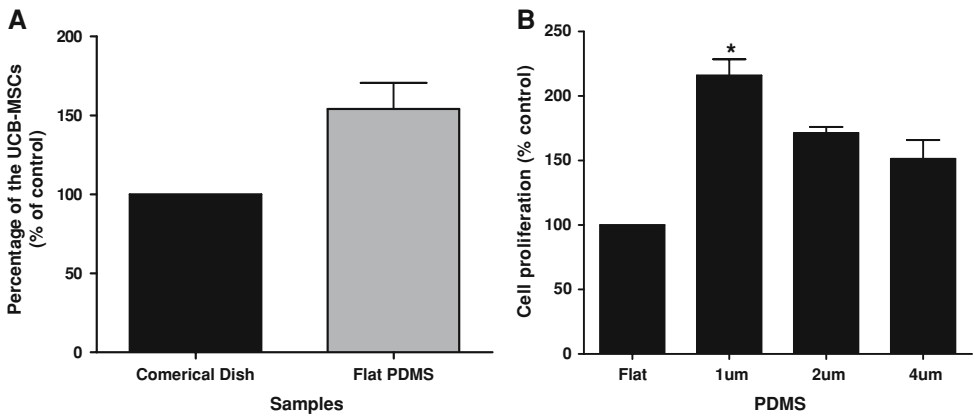


**Fig. 2** Proliferation of UCB-hMSCs on PDMS: (**a**) percentage of proliferating UCB-MSCs on flat PDMS and commercial dishes and (**b**) percentage of UCB-hMSCs in micro-scale fabricated PDMS (flat, 1, 2, and 4 μm). Values indicate the mean ± SD for 3–5 independent experiments ($P < 0.05$)

changed to medium containing 100 μm BHA and 1% DMSO in DMEM for 5 h. After the end of the treatment, to determine whether micro-patterned PDMS would affect neuronal differentiation of UCB-hMSCs, we assessed the immunoreactivity of β III tubulin, a neuron-specific marker, to determine differentiation into neural-like cells on micro-patterned PDMS. UCB-hMSCs were examined for differentiation into neuronal differentiation according to a previously reported method [21, 22]. Based on the immunostaining result (Fig. 5a, b), most of the UCB-hMSCs differentiated into neural-like cells on 1 μm-patterned PDMS. Differentiated neurons from UCB-hMSCs in flat PDMS were randomly distributed, and only few cells were expressed in β III tubulin. However, most of the cells on PDMS with 1 and 2 μm patterns showed high immunoreactivity with β III tubulin. In the control (flat PDMS), only 52% of UCB-hMSCs expressed the neuron marker, β III tubulin antibody. In contrast, UCB-hMSCs that differentiated into neural-like cells on patterned PDMS showed high immunoreactivity of β III tubulin antibody, except the PDMS with a 4 μm pattern. The smaller sizes of the micro-patterned PDMS induced significantly more neuronal differentiation of UCB-hMSCs. UCB-hMSCs were significantly differentiated into neurons and aligned along the 1 μm micro-patterned PDMS (80.25%). The PDMS with a 2 μm micro-pattern (72.50%) also increased neuronal differentiation of UCB-hMSCs. PDMS with a 4 μm micro-pattern showed similar immunoreactivity with β III tubulin and alignment with that occurring in flat PDMS, but without a significant effect, and the effects were lower than PDMS with 1 and 2 μm patterns. For quantification of the percentage of cells expressing β III tubulin, the number of

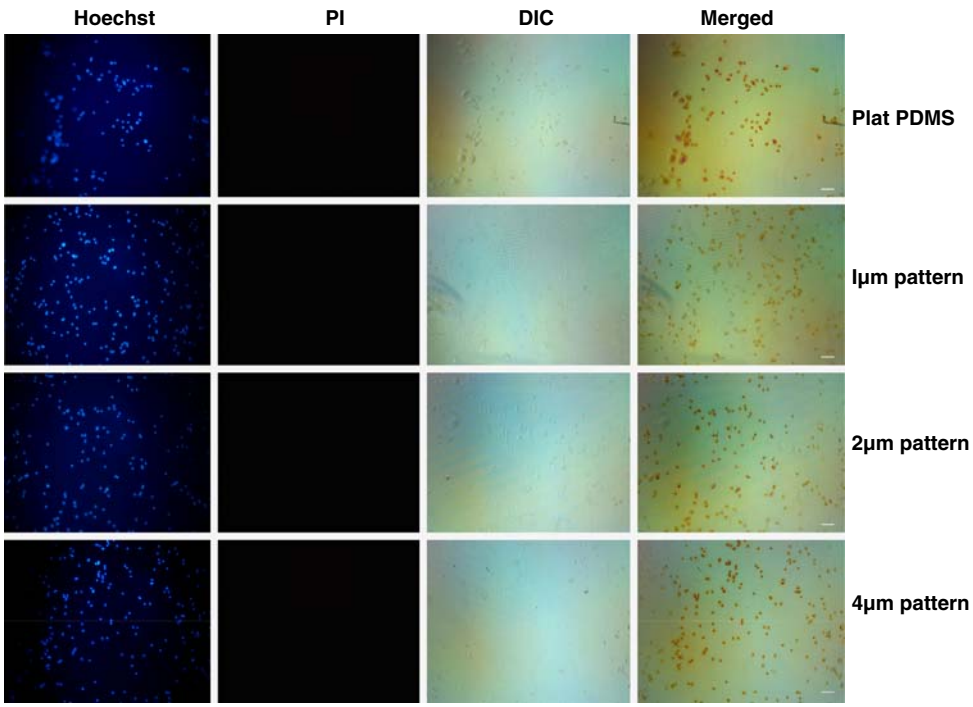


**Fig. 3** Co-staining of Hoechst 33238 and propidium iodide (PI). Hoechst 33238 and PI. Hoechst 33238 is a marker of apoptosis of cells with fragmented and/or condensed nuclei and PI is an indicator of necrotic cell death. Scale bar = 40 μm

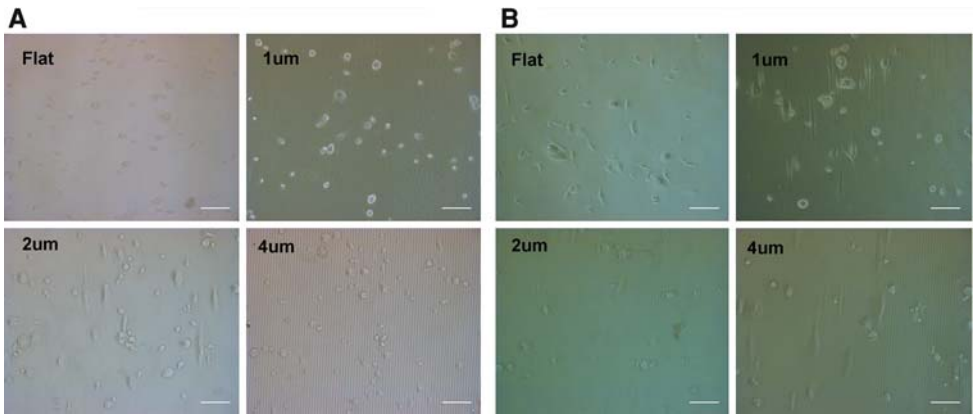


**Fig. 4** UCB-hMSCs differentiated into neural-like cells: (**a**) UCB-hMSCs on PDMS 24 h after seeding (before neuronal induction) and (**b**) UCB-hMSCs that were incubated in pre-neuronal induction medium (DMEM containing 1 mM BME and 5% FBS) for 24 h. Scale bar = 40 μm

positive cells was measured relative to total number of Hoechst 33238-labeled nuclei (Fig. 5c). We also examined other neuronal markers, thus differentiated neuronal cells on the PDMS were stained with microtubule associated protein 2 (MAP2) and neuronal nuclei (NeuN). As shown in Fig. 5e, immunoreactivity of MAP2 and NeuN was increased in most of the cells on PDMS with 1 μm patterns, but a few cells had immunoreactivity of MAP2 and NeuN protein in flat PDMS. Differentiated cells on the PDMS with a 2 μm micro-pattern also had more increased expression of MAP2 and NeuN than flat PDMS (Fig. 5f, g), whereas PDMS with a 4 μm micro-pattern showed the expression of MAP2 and NeuN protein similar to flat PDMS.

UCB-hMSCs were differentiated into neural-like cells at higher levels on micro-patterned PDMS than on flat PDMS. PDMS with 1 and 2 μm micro-patterns dramatically induced neural-like cells differentiation from UCB-hMSCs. Even though UCB-hMSCs were differentiated into neural-like cells on flat PDMS, only 50% of the UCB-hMSCs differentiated into neural-like cells, and this process was randomly directed (Fig. 5a–g).

### 3.4 Micro-patterned PDMS induced increased length of neuronal cells

To determine the lengths of the neural-like cells that differentiated from UCB-hMSCs, we measured the lengths of the neurons (Fig. 5d). We evaluated the ratio of the length of the differentiated neural-like cells in flat PDMS to those in micro-patterned PDMS. An increase in the length of neural-like cells was induced compared to that observed in

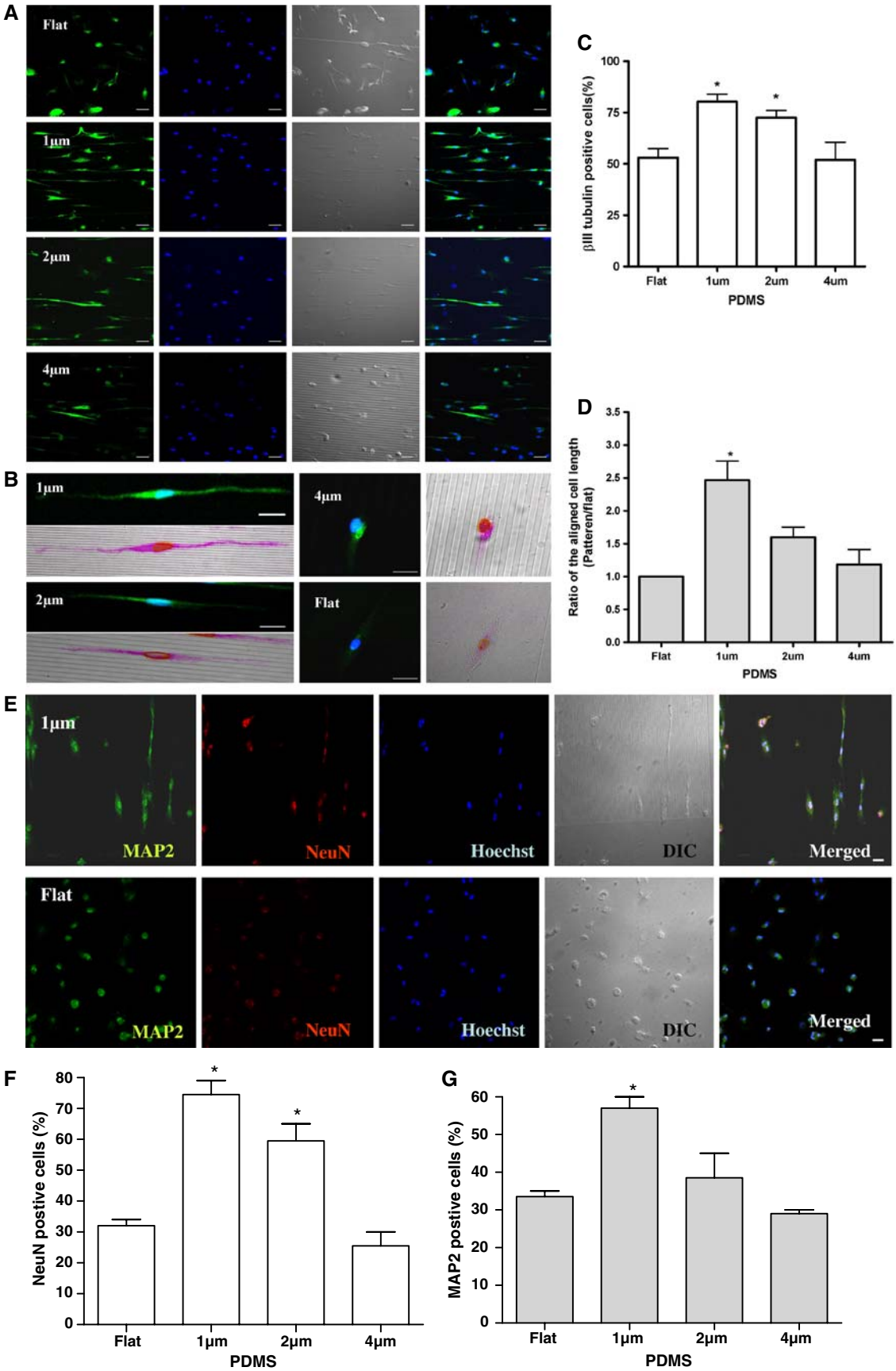
A
Flat
1μm
2μm
4μm
B
1μm
4μm
2μm
Flat
C
βIII tubulin positive cells(%)
100
75
50
25
0
Flat
1um
2um
4um
PDMS
D
Ratio of the aligned cell length (Patteren/flat)
3.5
3.0
2.5
2.0
1.5
1.0
0.5
0.0
Flat
1um
2um
4um
PDMS
E
1μm
MAP2
NeuN
Hoechst
DIC
Merged
Flat
MAP2
NeuN
Hoechst
DIC
Merged
F
NeuN postive cells (%)
80
70
60
50
40
30
20
10
0
Flat
1μm
2μm
4μm
PDMS
G
MAP2 postive cells (%)
60
50
40
30
20
10
0
Flat
1μm
2μm
4μm
PDMS

◀**Fig. 5** (**a**) Differentiated neural-like cells from UCB-hMSCs were analyzed by immunostaining with $\beta$ III tubulin (neuron marker, green) and Hoechst 33238 (nuclei marker, blue) in flat and micro-patterned PDMS. Scale bar = 40 μm. (**b**) A higher magnification of differentiated neuronal cells ($\beta$ III tubulin-positive cells) from UCB-hMSC on flat and micro-patterned PDMS. (**c**) Percentage of differentiated neural-like cells to non-neuronal cells derived from UCB-hMSCs (the $\beta$ III tubulin-positive cells/Hoechst 33238-positive cells) PDMS with 1 and 2 μm patterns induced significantly more immunoreactivity of $\beta$ III tubulin compared to flat PDMS. (**d**) Measurement length of UCB-hMSCs that differentiated into neuronal cells. Ratio of the length of the neuronal cells on PDMS flat to the length of the neural-like cells on micro-patterned PDMS. Lengths of the neural-like cells that differentiated from UCB-hMSCs were extended by the PDMS with 1 and 2 μm patterns. (**e**) MAP2 and NeuN expression of differentiated neural-like cells on PDMS with 1 μm and flat patterns. Scale bar = 20 μm. (**f**) Percentage of differentiated neural-like cells to non-neuronal cells derived from UCB-hMSCs (the NeuN-positive cells/Hoechst 33238-positive cells) PDMS. (**g**) Percentage of differentiated neural-like cells to non-neuronal cells derived from UCB-hMSCs (the MAP2-positive cells/Hoechst 33238-positive cells) PDMS. Values indicate the mean ± SD for 3–5 independent experiments ($P < 0.05$)

flat PDMS. PDMS with a 1 μm pattern increased the length of the neural-like cells to double that of the control, and the length of the neural-like cells was increased about 1.5-fold in PDMS with a 2 μm pattern. However, no difference in neuronal cell length was observed in 4 μm-patterned or flat PDMS.

### 3.5 Determination of differentiation into neuronal cell orientation on PDMS

To investigate whether the micro-patterned PDMS had effects on the alignment of the UCB-hMSCs that differentiated into neural-like cells, we measured the orientation of the differentiated neural-like cells on flat PDMS and the different widths of micro-patterned PDMS. We divided the micro-patterned PDMS into 10° sectors from 0 to 90°. The 0° represented perfect alignment to the fabricated micro-patterned PDMS. The orientation of differentiated neuronal cells from UCB-hMSCs was significantly influenced by the PDMS with a 1 μm pattern. In the differentiated neural-like cells, approximately 80% of the cells were aligned within 10° of the direction of the 1 μm micro-patterned PDMS (Fig. 6). In contrast, differentiation into neural-like cells in the control PDMS was not centralized at any specific degree of the angle, and was randomly distributed from 0 to 90° (Fig. 6).

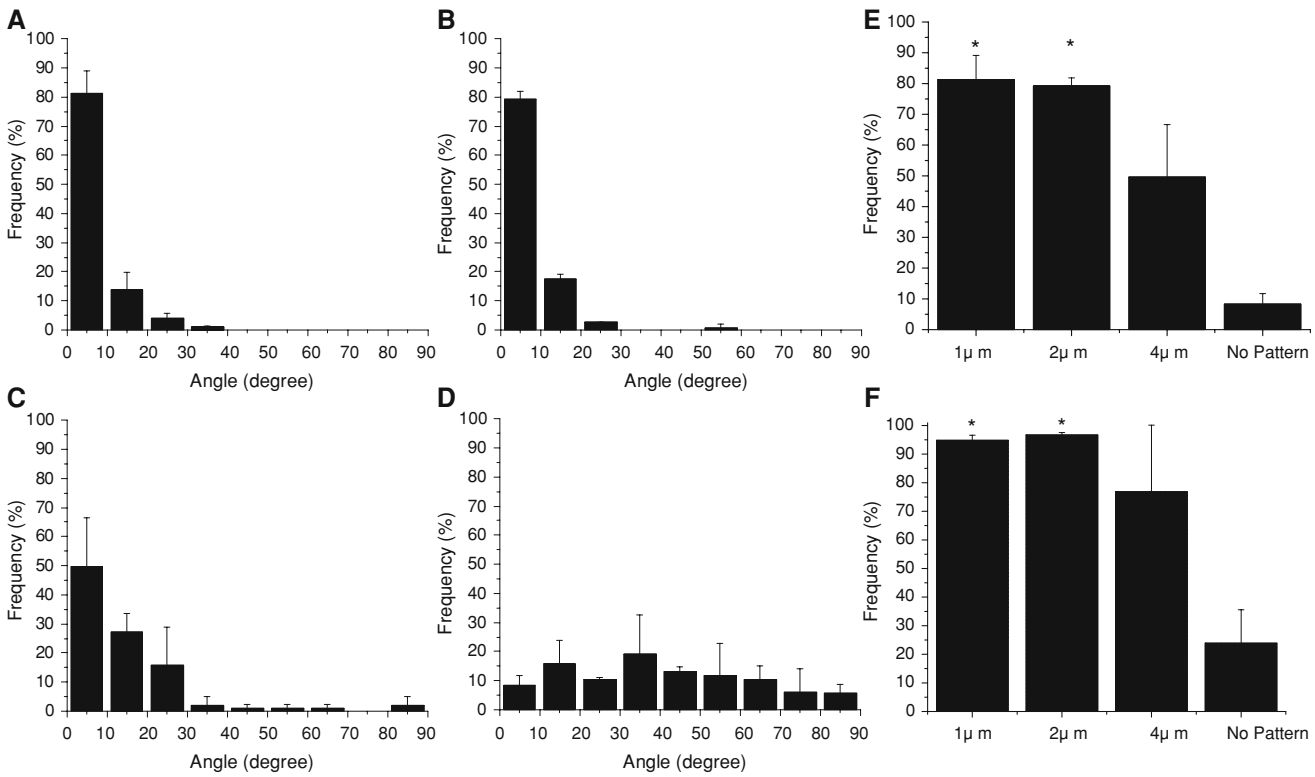


**Fig. 6** Distribution of the UCB-hMSCs differentiated neural-like cells on PDMS. (**a**) 1 μm, (**b**) 2 μm, (**c**) 4 μm, and (**d**) flat PDMS. We divided 10° sectors from 0 to 90°. Most of the differentiated neural-like cells were oriented within 10 and 20° of the angles in micro-patterned PDMS. Otherwise, on flat PDMS, cells were randomly distributed at all of the angles. The frequency of neuronal cells within 10° (**e**) and 20° (**f**), respectively. Values indicate the mean ± SD for 3–5 independent experiments ($P < 0.05$)

Additionally, we measured the frequencies of the cells aligned within 10 and 20° with respect to the grooves. Most of the differentiated neural-like cells in each different micro-patterned PDMS were significantly aligned within 10 or 20° (Fig. 6e, f). The differentiated neuronal cells in PDMS with a 2 μm pattern were mostly aligned within 20°, but more of the cells in PDMS with a 1 μm pattern were closely aligned to within 10°. The PDMS with 1 and 2 μm patterns had great effects on the linear alignment of the differentiation into neuronal cells, while PDMS with a 4 μm pattern and flat PDMS did not.

### 3.6 SEM image analysis

We performed SEM analysis to assess the images of the differentiation of UCB-hMSCs into neural-like cells in micro-patterned PDMS. This analysis showed that cells were aligned along the micro-pattern. However, as shown in Fig. 7a, the differentiated neuronal cells from UCB-hMSCs in flat PDMS were independently spread out, and the lengths of the cells tended to be short. Cells in PDMS with a 1 μm width pattern were extended to align along the micro-pattern (Fig. 7b, c). Differentiated neural-like cells in PDMS with a 4 μm pattern did not extend as much as those in PDMS with a 1 μm width pattern (Fig. 7f) or cells were aligned against micro-patterned PDMS (Fig. 7g).

### 3.7 Calcium response of differentiated neural-like cells on micro-patterned PDMS

To confirm whether micro-patterned PDMS could induce neuronal function of the differentiation into neural-like cells from UCB-hMSCs, we investigated differentiated cells by imaging calcium in response to high potassium chloride (KCl). Differentiated UCB-hMSCs on 1 μm-patterned PDMS induced an increase in calcium when 133 mM KCl was added for 50 s (Fig. 8a); differentiated UCB-hMSCs on 2 μm-patterned PDMS showed an increase in calcium, but not to the level of 1 μm-patterned PDMS (data not shown). Under the same conditions, differentiated neural-like cells from UCB-hMSCs in the 4 μm pattern (Fig. 8b) and flat PDMS (data not shown) did not increase the cytosolic calcium concentration. In accordance with immunostaining results, 1 and 2 μm-patterned PDMS not only enhanced the phenotype of the neural-like cell differentiation of UCB-hMSCs, but also increased the neuronal function.

## 4 Discussion

In this study, we investigated whether biomaterials and their physical guidance could affect the proliferation and

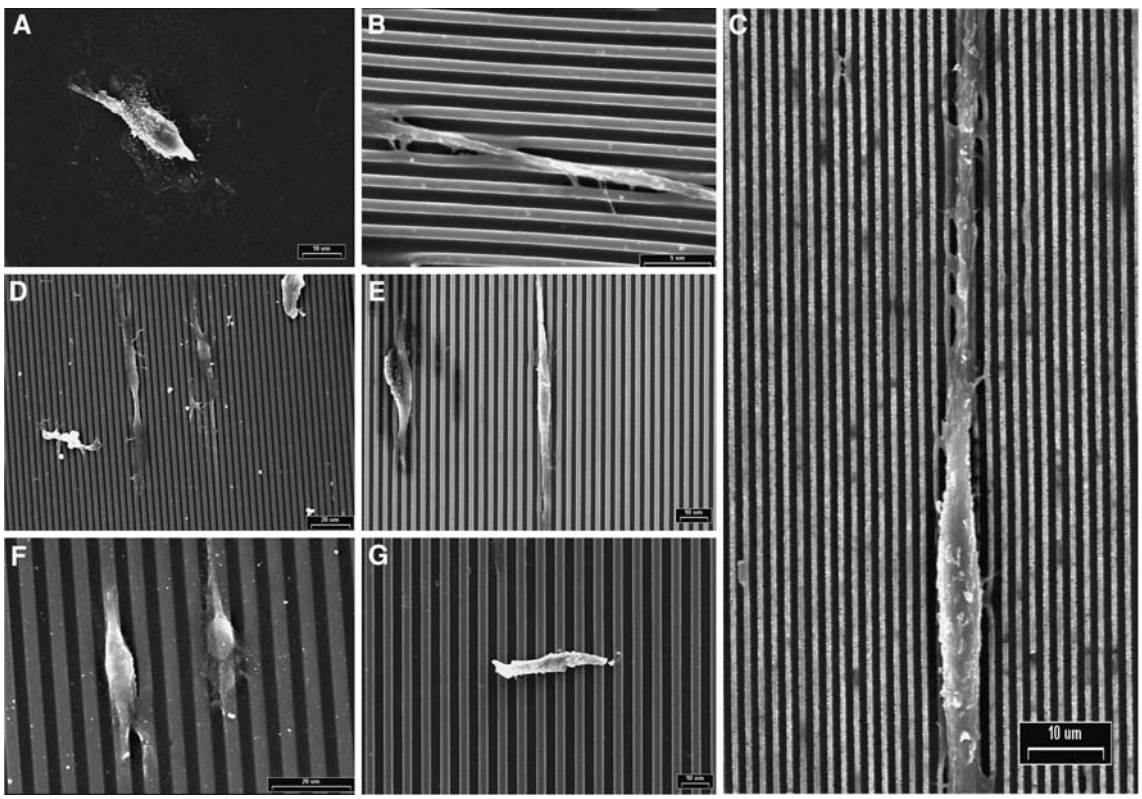


**Fig. 7** SEM image analysis. (**a**) Flat PDMS, (**b**, **c**) 1 μm, (**d**, **e**) 2 μm, and (**f**, **g**) 4 μm. After neural-like cells differentiation from UCB-hMSCs, we performed SEM analysis. (**a**, **c**, **e**, and **g**) scale = 10 μm; (**d**, **f**) scale = 20 μm; and (**b**) scale = 5 μm

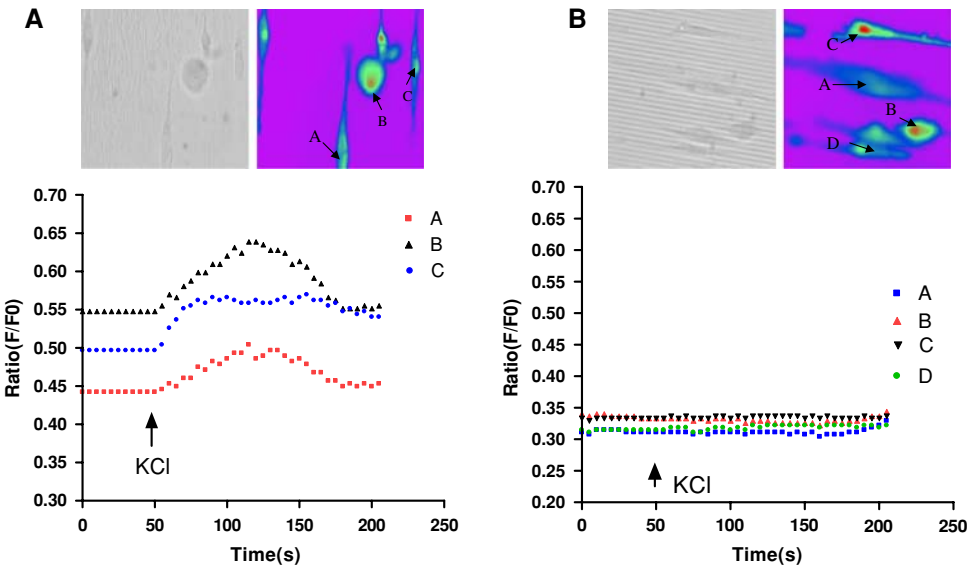


**Fig. 8** Calcium imaging. (**a**) Differentiated neuronal cells on PDMS with 1 μm pattern increased cytosolic calcium response when KCl (133 mM) was added for 50 s. (**b**) Differentiated neuronal cells on PDMS with 4 μm pattern had no response to KCl (133 mM) addition for 50 s. Response displayed by several characteristic cells (indicated by arrowheads). We performed 3–5 independent experiments

differentiation of UCB-MSCs. Recently, many studies have suggested that a number of biomaterials were useful for cell proliferation and differentiation, as well as tissue engineering [23–26].

We have shown that PDMS with a micro-pattern structure system has great potential to enhance differentiated neuronal cells from UCB-hMSCs. First, we tested cell proliferation on PDMS. The proliferation capacity of UCB-hMSCs was increased on flat PDMS, but there were not significant differences between the flat PDMS and commercial dishes. However, when the surface of PDMS was engraved in micro-scale, proliferation of UCB-hMSCs significantly increased and induced neural-like cell differentiation. We found that biomaterials themselves affected cell behavior, but we also determined that physical manipulation played a more important role in controlling cell growth and behavior. Among the micro-patterned PDMS samples, differentiated neural-like cells from UCB-hMSCs on the PDMS with a 1 μm width pattern showed an increase in neural-like cell differentiation of about 2-fold compared to the control (flat PDMS). Although 51% of UCB-hMSCs differentiated into neural-like cells in the 4 μm-patterned PDMS, there was no response to calcium movement as on the flat PDMS. Even though the UCB-MSCs exhibited 50% immunoreactivity with $\beta$ III tubulin, we presumed that they could not induce calcium increases due to the shortage of neurite outgrowth and the length of neurons. Many studies have demonstrated that the calcium channel has an important role in neurite outgrowth [27] and calcium influx into the growth cone processed through the voltage-operated and ligand-gated calcium channel [28, 29]. Differentiation into neural-like cells on flat or PDMS with a 4 μm pattern may have calcium channels, but insufficient to induce calcium influx. Moreover, the low expression of MAP2 and NeuN protein in flat PDMS showed that differentiated neural-like cells was not enough to differentiate mature neurons. Our results indicated that differentiated neural-like cells on 1 μm-patterned PDMS had neuronal function by increasing cytosolic calcium concentration. In addition, most of the differentiated neuronal cells on the 1 μm-patterned PDMS responded within 10° angles. The lengths of the differentiated neural-like cells were significantly higher in PDMS with a 1 μm pattern than in flat PDMS. Previously, researchers have reported that topographic and biological cues to increase neurite outgrowth and guidance of neural-like cells were crucial for randomly directed cells in order to facilitate regeneration and neuronal networks [19, 26, 30, 31] in neurologic injury. Various bridging devices, including biological substrates and biomaterial bridges have been used to promote neuronal regeneration in neurologic injury through the control of neural-like cell guidance [32, 33]. Control of orientation in UCB-hMSCs by micro-patterned PDMS induced directed neural-like cell growth and neuronal differentiation from UCB-hMSCs. These results have demonstrated that micro-patterned PDMS can induce neuronal differentiation and outgrowth to aid in regeneration in neurologic injury sites. PDMS was found to be an appropriate biomaterial in terms of physical modification, substrate for cell culture, and safety of implantation [34–36]. Our data suggest that PDMS is able to maximize stem cell therapy by controlling cell differentiation and orientation, as well as by inducing cell proliferation, and thus may be valuable in therapies for people who suffer with neurologic injury or disease. It is critical for stem cell-based therapeutic approaches to ensure complete differentiation of stem cells into the desired target cell type [37]. Our results indicate that combining biomaterials and physical cues are important factors in stem cell therapy to increase efficacy of treatment in diseases.

The molecular mechanism that affects the cell response in biomaterials with physical cues remains virtually unexplored. Therefore, we will investigate the molecular mechanisms that are involved in cell behavior and facilitating regeneration on PDMS with a micro-pattern. Moreover, we will investigate whether transplantation of stem cells engraved in micro-patterned PDMS can be utilized to induce efficient recovery from neurologic conditions in animal models. Taken together, these results indicate a promising method of combining stem cells and bioengineering to increase the positive effects of stem cell-based therapies. Our approaches will be applied to other neurologic diseases and will provide a powerful tool for regenerative medicine.

**Acknowledgements** This work was supported by the Seoul R&BD Program (#10548) and the BK (Brain Korea) 21 Program for Veterinary Science of Seoul National University, Republic of Korea, and the ERC grant from KOSEF through the Nano-bioelectronics and System Research Center of Seoul National University, Republic of Korea.

## References

1. K. Mareschi, I. Ferrero, D. Rustichelli, S. Aschero, L. Gammaitoni, M. Aglietta, E. Madon, F. Fagioli, J. Cell. Biochem. **97**, 744 (2006)
2. A. Erices, P. Conget, J.J. Minguell, Br. J. Haematol. **109**, 235 (2000)
3. M. Ryden, A. Dicker, C. Gotherstrom, G. Astrom, C. Tammik, P. Arner, K. Le Blanc, Biochem. Biophys. Res. Commun. **311**, 391 (2003)
4. X.Q. Kang, W.J. Zang, L.J. Bao, D.L. Li, X.L. Xu, X.J. Yu, Cell Biol. Int. **30**, 569 (2006)
5. Y.A. Romanov, A.N. Darevskaya, N.V. Merzlikina, L.B. Buravkova, Bull. Exp. Biol. Med. **140**, 138 (2005)
6. N.S. El-Badri, A. Hakki, S. Saporta, X. Liang, S. Madhusodanan, A.E. Willing, C.D. Sanberg, P.R. Sanberg, Stem Cells Dev. **15**, 497 (2006)
7. O.K. Lee, T.K. Kuo, W.M. Chen, K.D. Lee, S.L. Hsieh, T.H. Chen, Blood **103**, 1669 (2004)
8. S.W. Kim, H. Han, G.T. Chae, S.H. Lee, S. Bo, J.H. Yoon, Y.S. Lee, K.S. Lee, H.K. Park, K.S. Kang, Stem Cells **24**, 1620 (2006)
9. B. Sun, K.H. Roh, S.R. Lee, Y.S. Lee, K.S. Kang, Biochem. Biophys. Res. Commun. **354**, 919 (2007)
10. Y.S. Fu, Y.C. Cheng, M.Y. Lin, H. Cheng, P.M. Chu, S.C. Chou, Y.H. Shih, M.H. Ko, M.S. Sung, Stem Cells **24**, 115 (2006)
11. L. Roybon, N.S. Christophersen, P. Brundin, J.Y. Li, Cell Tissue Res. **318**, 261 (2004)
12. J.B. Recknor, J.C. Recknor, D.S. Sakaguchi, S.K. Mallapragada, Biomaterials **25**, 2753 (2004)
13. K.E. Schmalenberg, K.E. Uhrich, Biomaterials **26**, 1423 (2005)
14. J. Piantino, J.A. Burdick, D. Goldberg, R. Langer, L.I. Benowitz, Exp. Neurol. **201**, 359 (2006)
15. S.M. Rea, R.A. Brooks, A. Schneider, S.M. Best, W. Bonfield, J. Biomed. Mater. Res. **70**, 250 (2004)
16. L.J. Yang, Y.C. Ou, Lab Chip **5**, 979 (2005)
17. J.L. Charest, M.T. Eliason, A.J. Garcia, W.P. King, Biomaterials **27**, 2487 (2006)
18. E. Leclerc, A. Corlu, L. Griscom, R. Baudoin, C. Legallais, Biomaterials **27**, 4109 (2006)
19. M. Bani-Yaghoub, R. Tremblay, R. Voicu, G. Mealing, R. Monette, C. Py, K. Faid, M. Sikorska, Biotechnol. Bioeng. **92**, 336 (2005)
20. A. Mata, C. Boehm, A.J. Fleischman, G. Muschler, S. Roy, J. Biomed. Mater. Res. **62**, 499 (2002)
21. F.Z. Lu, M. Fujino, Y. Kitazawa, T. Uyama, Y. Hara, N. Funeshima, J.Y. Jiang, A. Umezawa, X.K. Li, J. Lab. Clin. Med. **146**, 271 (2005)
22. T. Tondreau, N. Meuleman, A. Delforge, M. Dejeneffe, R. Leroy, M. Massy, C. Mortier, D. Bron, L. Lagneaux, Stem Cells **23**, 1105 (2005)
23. Y.R. Shih, C.N. Chen, S.W. Tsai, Y.J. Wang, O.K. Lee, Stem Cells **24**, 2391 (2006)
24. T.M. Myckatyn, S.E. Mackinnon, J.W. McDonald, Transpl. Immunol. **12**, 343 (2004)
25. S. Sarkar, G.Y. Lee, J.Y. Wong, T.A. Desai, Biomaterials **27**, 4775 (2006)
26. J.B. Recknor, D.S. Sakaguchi, S.K. Mallapragada, Biomaterials **27**, 4098 (2006)
27. T.M. Gomez, J.Q. Zheng, Nat. Rev. **7**, 115 (2006)
28. B. Calabrese, S. Manzi, M. Pellegrini, M. Pellegrino, Eur. J. Neurosci. **11**, 2275 (1999)
29. Y. Li, Y.C. Jia, K. Cui, N. Li, Z.Y. Zheng, Y.Z. Wang, X.B. Yuan, Nature **434**, 894 (2005)
30. A.F. Ryan, J. Wittig, A. Evans, S. Dazert, L. Mullen, Audiol. Neurootol. **11**, 134 (2006)
31. S. Stokols, M.H. Tuszynski, Biomaterials **25**, 5839 (2004)
32. C.H. Chau, D.K. Shum, H. Li, J. Pei, Y.Y. Lui, L. Wirthlin, Y.S. Chan, X.M. Xu, FASEB J. **18**, 194 (2004)
33. T. Hadlock, C. Sundback, R. Koka, D. Hunter, M. Cheney, J. Vacanti, Laryngoscope **109**, 1412 (1999)
34. Y.S. Zinchenko, R.N. Coger, J. Biomed. Mater. Res. A **75**, 242 (2005)
35. S. Ostrovidov, J. Jiang, Y. Sakai, T. Fujii, Biomed. Microdevices **6**, 279 (2004)
36. C.J. Pino, F.R. Haselton, M.S. Chang, Cell Transplant. **14**, 565 (2005)
37. C. Chai, K.W. Leong, Mol. Ther. **15**, 467 (2007)